SCIENCE CHINA
Physics, Mechanics & Astronomy

•Article•

April 2022 Vol. 65 No. 4: 246111
https://doi.org/10.1007/s11433-021-1815-8

Correlation between boson peak and thermal expansion manifested by physical aging and high pressure

Rongjie Xue[1,2*], Linzhi Zhao[1], Yunqi Cai[1], Jiaojiao Yi[2], Jinguang Cheng[1], Ping Wen[1], Weihua Wang[1,3], Mingxiang Pan[1,4,5*], and Haiyang Bai[1,3*]

[1] *Institute of Physics, Chinese Academy of Sciences, Beijing 100190, China;*
[2] *School of Materials Engineering, Jiangsu University of Technology, Changzhou 213001, China;*
[3] *College of Materials Science and Opto-Electronic Technology, University of Chinese Academy of Sciences, Beijing 100049, China;*
[4] *School of Physical Sciences, University of Chinese Academy of Sciences, Beijing 100190, China;*
[5] *Songshan Lake Materials Laboratory, Dongguan 523808, China*

Received August 13, 2021; accepted November 22, 2021; published online January 24, 2022

We investigate the effects of high pressure and physical aging on the boson peak and thermal expansion of a typical metallic glass. Specifically, the thermal expansion coefficient and boson peak intensity monotonically decrease during physical aging. With the increase of high pressure, the boson peak intensity and the thermal expansion coefficient coincidently experience an incipient decrease and then a subsequent increase. The boson peak intensity shows an approximately linear relationship with the thermal expansion coefficient. The thermal expansion can be affected by structural relaxation or rejuvenation, which can reflect the flow units variation and atomic packing of a metallic glass. Our results indicate a direct link between structural relaxation or rejuvenation and fast boson peak dynamics, providing insights into the boson peak behavior and structural heterogeneity of metallic glasses.

metallic glass, thermal expansion, boson peak, high pressure, aging

PACS number(s): 61.43.Dq, 61.20.Lc, 62.50.+p, 61.72.Cc, 65.60.+a

Citation: R. Xue, L. Zhao, Y. Cai, J. Yi, J. Cheng, P. Wen, W. Wang, M. Pan, and H. Bai, Correlation between boson peak and thermal expansion manifested by physical aging and high pressure, Sci. China-Phys. Mech. Astron. **65**, 246111 (2022), https://doi.org/10.1007/s11433-021-1815-8

1 Introduction

Glassy materials possess distinctive properties at low temperatures in comparison with their crystalline counterparts [1,2]. One of the low temperature properties of glasses is the "boson peak", which is in the terahertz region in the vibrational spectrum and can be reflected in heat capacity C_p by a maximum over the Debye T^3 law in the temperature T dependence of C_p/T^3 at approximately 10 K [1]. This universal feature of glasses is the low-frequency enhancement of vibrational density of states as compared with the Debye law [1,2]. Several models have been proposed to explain the low-frequency excited states. Such models include elastic heterogeneities [3-6], strongly anharmonic transition between minima-dominated phase and the saddle-dominated phase of the energy landscape [2,7], soft anharmonic potentials [8,9], interstitialcy-like "defects" [10], smeared out van Hove singularities [11,12], and structural parameter of "orientational order" [13]. These models are commonly related to the spatially heterogeneous distributed regions contributing to the excess vibrational density of states. Metallic glass (MG) with the dense random packing of hard spheres structure [14-

*Corresponding authors (Rongjie Xue, email: xuerongjie@jsut.edu.cn; Mingxiang Pan, email: panmx@iphy.ac.cn; Haiyang Bai, email: hybai@iphy.ac.cn)

17] is considered as a relatively simple glass to study this controversial issue in glass science [18-20]. Intensive investigations suggest that the boson peak has correlations with shear bands [18,19] and β-relaxation [20] in MGs. It has been implied that the boson peak in MGs originates from the defective nano soft regions linked to the transverse vibrational modes [18-21] or localized Einstein-type vibration harmonic model [20,22,23]. However, the nature of the boson peak in MGs remains controversial.

In general, MGs naturally relax to a lower energy state by annihilating the defects of free volumes or flow units [19,24,25]. By contrast, MGs can also be rejuvenated to high energy states originating from defects of negative free volumes or negative flow units via various mechanical and thermal treatments [26-28]. Thermal expansion is an intrinsic feature of MGs and involves anharmonic atomic vibrations [29], which can be affected by various mechanical and thermal processes [30,31]. Previous studies on the thermal expansion of MGs focused on the effects of relaxation or crystallization [30-32], whereas few studies pay close attention to the evolution of thermal expansion via high pressure treatment [30]. Comparing with the thermal expansion, some efforts have been exerted to understand the dynamic behaviors of the boson peak under high pressure treatment, but the pressure is lower [33-35]. Simulations and experimental studies reported that the boson peak is correlated with the structural relaxation manifested by a negative relationship between the fragility of the glass-forming liquids and the boson peak intensity of MGs [21], and a positive relationship between the relative enthalpy change and the boson peak intensity of MGs [25]. However, whether the correlation between the thermal expansion and the boson peak is significant in MGs remains unclear. Establishing this relationship can help us further demonstrate the possible link between structural relaxation or rejuvenation and boson peak in MGs and provide insights into the boson peak behavior and structural heterogeneity of MGs.

In this work, we trace the evolutions of boson heat capacity peak and thermal expansion under high pressure and physical aging. Results show that the linear thermal expansion coefficient and the boson peak intensity monotonically decrease toward the equilibrium of the metastable state upon physical aging at a constant temperature. The linear thermal expansion coefficient and the boson peak intensity of the MGs show an obvious nonmonotonic behavior but in the same changing tendency with increasing pressure under high pressure at room temperature. The linear thermal expansion coefficient shows an approximately linear relationship with the boson peak intensity. The significant correlation between the boson peak and the thermal expansion indicates a direct link between the structural relaxation or rejuvenation and the boson peak dynamics, which bring a new insight into the dynamic behaviors and structural heterogeneity of MGs.

2 System and experimental methods

$Pd_{40}Ni_{10}Cu_{30}P_{20}$ bulk MG was prepared by sucking the master alloy ingot into a water-cooled copper mold to obtain cylindrical rods. The glassy nature of the samples was confirmed via X-ray diffraction and differential scanning calorimetry (DSC). The as-cast MGs were heated to the supercooled liquid and then cooled down to room temperature (RT) at 60 K/min by DSC to obtain the standard MGs. The standard MGs were subjected to high pressure experiments using a hexahedral anvil and a 6/8 two-stage pressurized high pressure apparatus and then held under quasi-hydrostatic pressure for 1 h at RT [36]. The as-cast MGs were isothermally annealed at $0.85T_g$ (the glass transition temperature T_g and crystallization temperature T_x at a heating rate of 20 K/min were 566 and 653 K, respectively) for various times under a vacuum of $\sim 1\times10^{-5}$ Pa in a furnace, respectively, and then cooled down to RT for the further measurements. The linear thermal expansion coefficient (α) was measured through thermo-mechanical analysis (Netzsch TMA 402F3) at a heating rate of 5 K/min in a compression mode with an applied force of 30 mN. The low temperature heat capacity C_p was measured from 2 to 100 K using the Quantum Design physical property measurement system (PPMS 6000). ^{63}Cu nuclear magnetic resonance (NMR) experiments were performed using a Bruker Avance Ⅲ 400 HD spectrometer with a 9.39 T magnetic field at RT. ^{63}Cu NMR spectra of the powdered samples (standard and high pressure-treated MGs were broken into powders) were obtained through Fourier transformation of spin-echo signals. Hahn echo pulse sequence was used with a typical pulse delay for the glassy alloys of 150 ms, and the time between the first and second pulses was set to 10 μs. The first pulse length was set to 3.35 μs. All ^{63}Cu NMR shifts were referenced to CuCl powders (−332 ppm at RT).

3 Results and discussion

The evolution of the thermal expansion and boson heat capacity peak in the MGs during high pressure and physical aging was compared. Figure 1 shows the measured low temperature heat capacity as $(C_p-C_p^{cryst})/T^3$ versus T for the standard, high pressure-processed, as-cast, and aged MGs, making a visible contribution of the boson peak. C_p and C_p^{cryst} represent the experimentally measured low temperature heat capacity of the various processed MGs and the $Pd_{40}Ni_{10}Cu_{30}P_{20}$ crystalline counterpart, respectively. C_p^{cryst} is a crucial heat capacity from electronic and lattice contributions but has no contribution to the boson peak. Therefore, it is used as a reference and subtracted from the low temperature heat capacity of the MGs to make an obvious boson peak contribution. Figure 1(a) presents the bo-

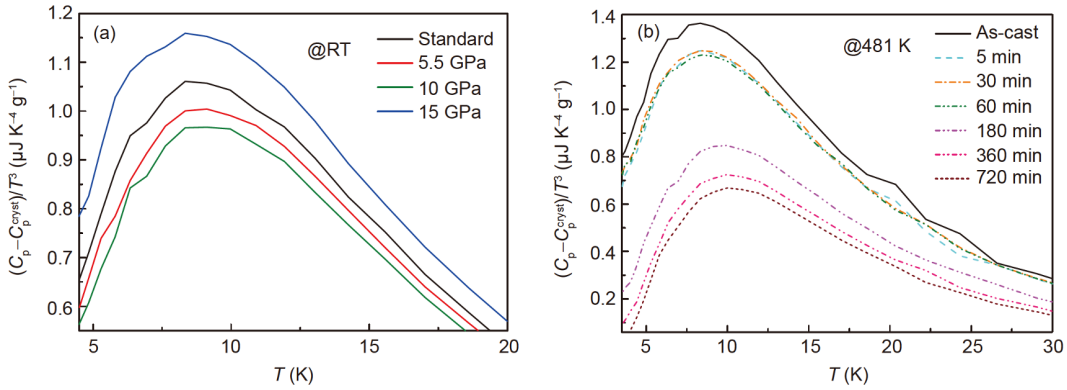

Figure 1 (Color online) Evolution of boson heat capacity peaks of Pd-based MGs. Samples were (a) processed under high pressure at RT for different quasi-hydrostatic pressures and (b) annealed by physical aging at 481 K for various aging times.

son peak evolution of the MGs under high pressure. The boson peak becomes increasingly depressed with increasing pressure. However, when the pressure is over 10 GPa, the boson peak is much enhanced and pronounced than that of the standard MG. The peak shifts to higher temperature with pressure increasing from ambient pressure to 10 GPa, and shifts to lower temperature when the pressure increases to 15 GPa. Such pressure effect on the boson peak is not analogous to previous studies [33-35]. This discrepancy might be due to the fact that the pressure applied on the MGs is much higher than theirs. Figure 1(b) shows the boson peak evolution of the MGs during physical aging. The boson peak becomes increasingly depressed, and the peak shifts to higher temperature with increasing annealing time, showing a monotonic evolution tendency. After 180 min of annealing, the boson peak intensity and position show relatively small changes and gradually approach the saturation value. When the annealing time is infinitely long, the boson peak intensity and position approach the equilibrium value of this annealing temperature [25]. The aging effect on the boson peak agrees with previous studies observed in other MGs [18,19,25]. For both high pressure and physical aging, it conforms that the higher strength of the boson peak, the peak maximum occurs at the lower temperature.

The typical curves of the relative length change (ΔL and L_0 are the length change and the initial length of the MGs, respectively) versus T of the standard, high pressure-processed, as-cast, and aged MGs are shown in Figure 2. The relative length change $\Delta L/L_0$ increases with temperature up to the glass transition temperature and then rapidly decreases until crystallization because of a softening caused by viscous creep driven by the applied stress [32,37,38]. We focus on the relative length change of the MGs before glass transition. Under high pressure at RT (Figure 2(a)), the relative length change curve of the MG shifts down with increasing pressure, then rises up when the external quasi-hydrostatic pressure increases over 10 GPa, and the slope of the relative length change curve changes from gentler to steeper. During the physical aging (inset of Figure 2(b)), as the aging time increases, the relative length change curve of the MG gradually shifts down, and the slope becomes smaller and gentler (see Figure 2(b)), showing a typical structural relaxation of MGs [32,39,40]. The relative length change of the MGs is more sensitive to pressure, showing a non-

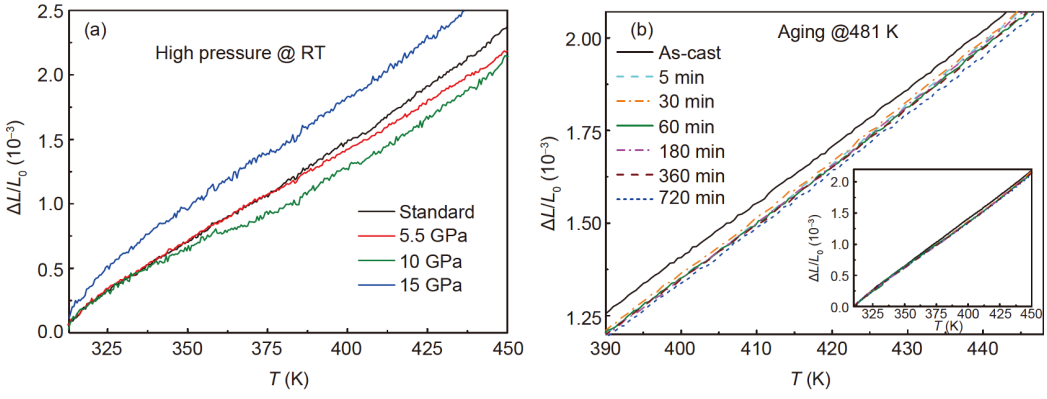

Figure 2 (Color online) Relative length changes of MGs after (a) high pressure treatment for various quasi-hydrostatic pressures at RT and (b) physical aging at 481 K for various aging times shown from 390 to 448 K. Inset in (b) is the typical curves of the relative length change versus T of the as-cast and aged MGs.

monotonic evolution behavior, while it monotonically decreases toward the equilibrium value during isothermal physical aging.

The linear thermal expansion coefficient $\alpha=\Delta L/(L_0\times\Delta T)$ is the slope of the relative length change curve taken from 313 to 448 K [29]. Figure 3 compares the evolution of the boson peak height (peak maximum of $(C_p-C_p^{cryst})/T^3$) and the linear thermal expansion coefficient α vs. aging time (Figure 3(a)) and pressure (Figure 3(b)). Figure 3(a) plots that the α and the boson peak height decrease with prolonged aging time, and the most change occurs in the first 30 min. During physical aging, the α and the boson peak height behave the same decrease monotonically evolution, showing a typical structural relaxation behavior. However, when various pressures were applied on the standard MG samples, the thermal expansion and the boson peak exhibit different behaviors (see Figure 3(b)). The pressure dependent α initially decreases and then increases to a value that surpasses the original value (see square dots in Figure 3(b)). Figure 3(b) shows the surprising results that the pressure dependent boson peak height initially decreases to a minimum and then increases to a maximum, which is consistent with the tendency of α. For the circle dots, with 15 GPa at RT, the boson peak height value is higher than the initial value, which agrees with α under the same pressure treatment. The magnitude of the boson peak and the linear thermal expansion coefficient α follow a similar evolution for physical aging and high pressure treatment. As a consequence, after high pressure or physical aging, the boson peak reflecting the anomalous atomic vibration in the frequency spectra of MGs behaves akin to the thermal expansion measurements. The inset of Figure 3 plots the boson peak height vs. the linear thermal expansion coefficient α. Within the accuracy limit of the method of measuring the thermal expansion and boson peak behaviors, the boson peak intensity exhibits an almost linear relationship with the linear thermal expansion coefficient. Another important parameter associated with the boson peak is the boson peak temperature, which can also characterize the correlation between the boson peak and the thermal expansion. In addition, similar linear relationship results can be found between the boson peak temperature and the linear thermal expansion coefficient. The results show a quantitative construction of the correlation between the thermal expansion and the boson peak. The boson peak height is in line with the linear thermal expansion coefficient α during not only high pressure but also physical aging, indicating a clear correlation between the thermal expansion and dynamic behavior of the boson peak in the MGs.

Simulation results show that the transverse vibrational modes associated with local low-density defective structures contribute to the vibrational density of states or the boson peak [21]. Recently, experimental and simulation results have revealed that the soft local structure with excess free volume enhances the boson contribution to the heat capacity of MGs [18-23]. Previous studies also proved that defects with excess free volume and low energy play a significant role in thermal expansion [39,40]. Structural relaxation or aging is due to the microstructural heterogeneity of MGs and can be attributed to the movement of loose packing atoms in the liquid-like soft regions or "flow units" [16,24,25,41-43]. The boson peak and thermal expansion are related to the soft localized regions or flow units [20-23,25,39,40]. Recent X-ray photo correlation spectroscopy studies of MGs provide an atomic scale microstructure map for aging that affects the density until the density heterogeneities are released completely [44]. On the basis of these scenarios, a microscopic picture of the boson peak and thermal expansion of the physical aging effect can be drawn. The flow units where the atoms pack loosely and have higher potential energies can easily be activated via thermal treatments. The rearrangement and energy dissipation of atoms in flow units result in structural relaxation behaviors caused by annealing. Physical aging actually leads to an evolution of the annihilation of flow units and a relatively microscopic homogeneous state of MGs [24,25,41,42], resulting in the observed monotonic decrease in linear thermal expansion coefficient and boson

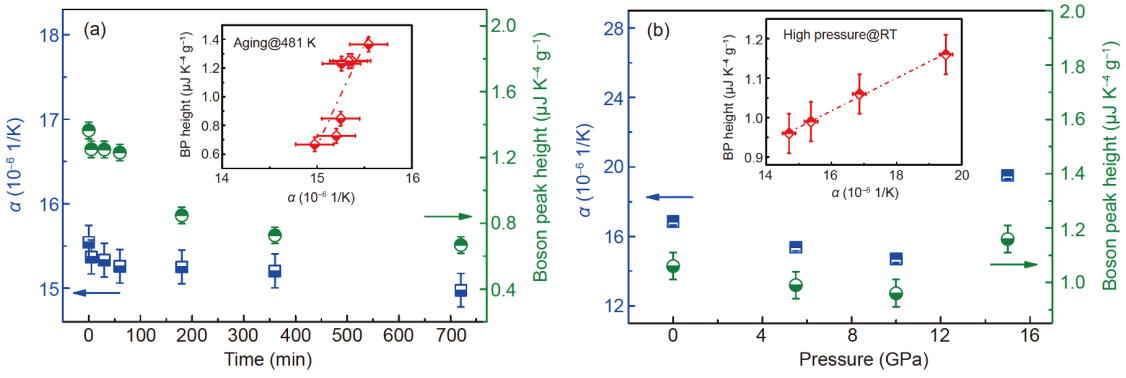

Figure 3 (Color online) Boson peak height (circle dots) and linear thermal expansion coefficient α (square dots) against (a) the time for physical aging at 481 K and (b) quasi-hydrostatic pressure for high pressure at RT. Insets in (a) and (b) show the relationship between the boson peak height and the linear thermal expansion coefficient; data from physical aging (a) and high pressure (b) are embraced. The dashed line serves as a guide for the eyes.

peak intensity. Conjecturally, the annihilation of defects of flow units contributes to the consistent changing tendency of the thermal expansion coefficient and boson peak intensity during physical aging.

The relationship between the boson peak and thermal expansion under high pressure is similar to but slightly different from that under physical aging (see Figure 3). Experimental results indicate that pressure, similar to temperature, is liable to induce atomic rearrangement as well [28,30,31,35,36]. Recent simulation results indicate that the pressure can change the atomic configuration, e.g., icosahedra and defects of soft regions of MGs [45,46]. The local site symmetry and electronic properties of MGs were studied by ^{63}Cu NMR spectroscopy [36,47,48], which can reflect the effect of structural change of MGs on the thermal expansion and the boson peak. Figure 4 plots the ^{63}Cu NMR spectra of the standard and high pressure-processed MGs. The peak position of the symmetrical central line can represent the isotropic Knight shift of the MGs. Previous experimental results prove that the structural change of MGs can be reflected by the change of Knight shift [47,48]. With increasing pressure, the ^{63}Cu isotropic Knight shift decreases from 785 ppm for the standard MG to 735 ppm for the high pressure-processed MG under 10 GPa, resulting in the observed decrease in linear thermal expansion coefficient and boson peak intensity. At a higher pressure of 15 GPa, the ^{63}Cu isotropic Knight shift increases to 840 ppm, which is larger than the initial value. Thus, an increase linear thermal expansion coefficient and boson peak intensity behavior were observed. The results demonstrate that the distribution of local atoms at ^{63}Cu sites is changed by high pressure that similar to the simulation results [46], indicating that the changes of atomic configurations of the MGs contribute to the thermal expansion and the boson peak behaviors. The evolution of the Knight shift in Figure 4 further confirms that the structures of the MGs are similar below 10 GPa but significantly different from those above 10 GPa. The critical change in Knight shift at approximately 10 GPa demonstrates that the distribution of local atoms at ^{63}Cu sites below 10 GPa is distinct from that above 10 GPa, indicating that the critical change of structure of MG has been changed around 10 GPa.

Experimental results show that high pressure is an effective and controllable way to alter the properties and energy states of MGs, indicating that the changes of local soft localized region structures and the bonding states between atoms are the microstructural origins [28,30,33-36]. It is widely accepted that the local defect atoms vibrations contribute to the boson peak and thermal expansion of MGs [2,6,10,20-22,25,26,30-32]. Thus, the behaviors of thermal expansion and boson peak during high pressure procedure can be interpreted. When the pressure is low, pressure promotes the atoms in loosely packed liquid-like regions re-

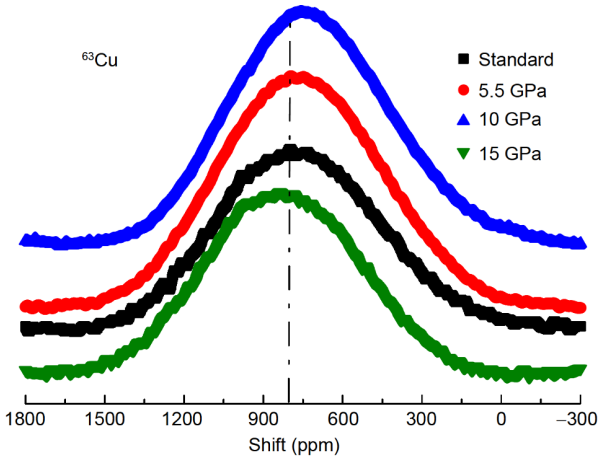

Figure 4 (Color online) NMR spectra of standard and high pressure-processed (5.5, 10, and 15 GPa) MGs.

arrangement and efficiently packing [28,30,36]. It also changes the width of the interatomic distance distribution and thereby lowers the thermal expansion and boson peak. The flow units annihilation dominates the process and results in structural relaxation when the pressure is lower than 10 GPa [28,30,36]. Nevertheless, when the pressure is over 10 GPa, the MG is greatly compressed, and the atoms rearrange into a high packing density configuration [25-28,30,31], leading to a higher thermal expansion coefficient and boson peak intensity and resulting in rejuvenation. Experimental and simulation studies have confirmed that the rejuvenated MG induced by high pressure originates from the microstructural change that involves negative flow units with a higher atomic packing density [28,46]. Combining with the Lennard-Jones-like potential, the phenomena can be further understood. With the pressure increasing up to 10 GPa, the interatomic distance decreases toward the critical distance located at the bottom of the potential well, resulting in the defects of flow units shrinkage and annihilation that correspond to structural relaxation. When the pressure further increases over 10 GPa, the interatomic distance decreases and go across the bottom of the potential well, leading to a higher potential energy and a more densification structure of MGs that corresponds to rejuvenation [25-28,30,31]. With increasing pressure, the flow units change from positive to zero and finally to a negative value that contributes to the nonmonotonic changes of the boson peak and the thermal expansion coefficient. When the pressure reaches approximately 10 GPa, the local structure of flow units with low packing density and low coordination changes to negative flow units with high atomic packing density and high coordination, which could be the structural origin of the extraordinary nonmonotonic phenomenon. From these points of view, the intrinsically universal correlation between the thermal expansion and the boson peak indicates that the structural relaxation or rejuvenation is

closely linked with the boson peak, and the local defective microstructure is its structural origin [20-23,25-30,38,40].

4 Conclusion

Using high pressure and physical aging methods, we report the evolution of thermal expansion and boson peak and then sequentially bridge the structural relaxation/rejuvenation and the boson peak in a typical Pd-based MG. The monotonic and nonmonotonic boson peak evolution behaviors have been observed under physical aging and high pressure respectively, and the thermal expansion shows the similar evolution tendency. The results indicate a close correlation between the slow structural relaxation or rejuvenation and fast boson peak dynamics. It benefits the understanding of the anomalous low-frequency excited states and the heterogeneous nature of MGs.

This work was supported by the National Natural Science Foundation of China (Grant Nos. 51801083, 11790291, 51461165101, 51801124, and 51671211), and the Natural Science Foundation of Jiangsu Province (Grant No. BK20181044).

1 W. A. Phillips, *Amorphous Solids: Low-Temperature Properties* (Springer, Berlin, 1981).
2 T. S. Grigera, V. Martín-Mayor, G. Parisi, and P. Verrocchio, Nature **422**, 289 (2003).
3 N. Tomoshige, S. Goto, H. Mizuno, T. Mori, K. Kim, and N. Matubayasi, J. Phys.-Condens. Matter **33**, 274002 (2021).
4 A. Giuntoli, and D. Leporini, Phys. Rev. Lett. **121**, 185502 (2018).
5 L. Zhang, J. Zheng, Y. Wang, L. Zhang, Z. Jin, L. Hong, Y. Wang, and J. Zhang, Nat. Commun. **8**, 67 (2017).
6 S. Gelin, H. Tanaka, and A. Lemaître, Nat. Mater. **15**, 1177 (2016).
7 V. Lubchenko, and P. G. Wolynes, Proc. Natl. Acad. Sci. USA **100**, 1515 (2003).
8 U. Buchenau, Y. M. Galperin, V. L. Gurevich, D. A. Parshin, M. A. Ramos, and H. R. Schober, Phys. Rev. B **46**, 2798 (1992).
9 V. L. Gurevich, D. A. Parshin, and H. R. Schober, Phys. Rev. B **67**, 094203 (2003).
10 V. A. Khonik, Chin. Phys. B **26**, 016401 (2017).
11 S. N. Taraskin, Y. L. Loh, G. Natarajan, and S. R. Elliott, Phys. Rev. Lett. **86**, 1255 (2001).
12 A. Chumakov, G. Monaco, A. Fontana, A. Bosak, R. Hermann, D. Bessas, B. Wehinger, W. Crichton, M. Krisch, R. Rüffer, G. Baldi, G. Carini Jr., G. Carini, G. D'Angelo, E. Gilioli, G. Tripodo, M. Zanatta, B. Winkler, V. Milman, K. Refson, M. Dove, N. Dubrovinskaia, L. Dubrovinsky, R. Keding, and Y. Yue, Phys. Rev. Lett. **112**, 025502 (2014).
13 J. Yang, Y. J. Wang, E. Ma, A. Zaccone, L. H. Dai, and M. Q. Jiang, Phys. Rev. Lett. **122**, 015501 (2019).
14 A. Meyer, Phys. Rev. B **66**, 134205 (2002).
15 D. B. Miracle, Acta Mater. **61**, 3157 (2013).
16 Z. Wang, and W. H. Wang, Natl. Sci. Rev. **6**, 304 (2019).
17 K. Zhao, Z. Bai, L. Zhang, and G. Liu, Sci. China-Phys. Mech. Astron. **60**, 106121 (2017).
18 J. Bünz, T. Brink, K. Tsuchiya, F. Meng, G. Wilde, and K. Albe, Phys. Rev. Lett. **112**, 135501 (2014).
19 Y. P. Mitrofanov, M. Peterlechner, S. V. Divinski, and G. Wilde, Phys. Rev. Lett. **112**, 135901 (2014).
20 B. Huang, Z. G. Zhu, T. P. Ge, H. Y. Bai, B. A. Sun, Y. Yang, C. T. Liu, and W. H. Wang, Acta Mater. **110**, 73 (2016).
21 H. Shintani, and H. Tanaka, Nat. Mater. **7**, 870 (2008).
22 M. B. Tang, H. Y. Bai, and W. H. Wang, Phys. Rev. B **72**, 012202 (2005).
23 Y. Li, H. Y. Bai, W. H. Wang, and K. Samwer, Phys. Rev. B **74**, 052201 (2006).
24 R. J. Xue, L. Z. Zhao, M. X. Pan, B. Zhang, and W. H. Wang, J. Non-Crystal. Solids **425**, 153 (2015).
25 P. Luo, Y. Z. Li, H. Y. Bai, P. Wen, and W. H. Wang, Phys. Rev. Lett. **116**, 175901 (2016).
26 G. Ding, C. Li, A. Zaccone, W. H. Wang, H. C. Lei, F. Jiang, Z. Ling, and M. Q. Jiang, Sci. Adv. **5**, eaaw6249 (2019).
27 S. V. Ketov, Y. H. Sun, S. Nachum, Z. Lu, A. Checchi, A. R. Beraldin, H. Y. Bai, W. H. Wang, D. V. Louzguine-Luzgin, M. A. Carpenter, and A. L. Greer, Nature **524**, 200 (2015).
28 C. Wang, Z. Z. Yang, T. Ma, Y. T. Sun, Y. Y. Yin, Y. Gong, L. Gu, P. Wen, P. W. Zhu, Y. W. Long, X. H. Yu, C. Q. Jin, W. H. Wang, and H. Y. Bai, Appl. Phys. Lett. **110**, 111901 (2017).
29 N. W. Ashcroft, and N. D. Mermin, *Solid State Physics* (Saubders College Publishing, New York, 1976).
30 R. Yamada, Y. Shibazaki, Y. Abe, W. Ryu, and J. Saida, Sci. Rep. **10**, 7438 (2020).
31 J. Guo, S. Joo, D. Pi, W. Kim, Y. Song, H. S. Kim, X. Zhang, and D. Kong, Adv. Eng. Mater. **21**, 1800918 (2018).
32 N. Mattern, J. Bednarcik, M. Stoica, and J. Eckert, Intermetallics **32**, 51 (2013).
33 V. L. Gurevich, D. A. Parshin, and H. R. Schober, Phys. Rev. B **71**, 014209 (2005).
34 K. Niss, B. Begen, B. Frick, J. Ollivier, A. Beraud, A. Sokolov, V. N. Novikov, and C. Alba-Simionesco, Phys. Rev. Lett. **99**, 055502 (2007).
35 L. Hong, B. Begen, A. Kisliuk, S. Pawlus, M. Paluch, and A. P. Sokolov, Phys. Rev. Lett. **102**, 145502 (2009).
36 R. J. Xue, L. Z. Zhao, C. L. Shi, T. Ma, X. K. Xi, M. Gao, P. W. Zhu, P. Wen, X. H. Yu, C. Q. Jin, M. X. Pan, W. H. Wang, and H. Y. Bai, Appl. Phys. Lett. **109**, 221904 (2016).
37 J. C. Bendert, M. E. Blodgett, A. K. Gangopadhyay, and K. F. Kelton, Appl. Phys. Lett. **102**, 211913 (2013).
38 H. Kato, H. S. Chen, and A. Inoue, Script. Mater. **58**, 1106 (2008).
39 N. Mattern, M. Stoica, G. Vaughan, and J. Eckert, Acta Mater. **60**, 517 (2012).
40 J. Steinberg, S. Tyagi, and A. E. Lord Jr., J. Non-Crystal. Solids **41**, 279 (1980).
41 J. C. Mauro, S. S. Uzun, W. Bras, and S. Sen, Phys. Rev. Lett. **102**, 155506 (2009).
42 R. Richert, Phys. Rev. Lett. **104**, 085702 (2010).
43 W. X. Jiang, and B. Zhang, Sci. China-Phys. Mech. Astron. **57**, 1870 (2014).
44 V. M. Giordano, and B. Ruta, Nat. Commun. **7**, 10344 (2016).
45 J. Ding, M. Asta, and R. O. Ritchie, Phys. Rev. B **93**, 140204 (2016).
46 N. Miyazaki, M. Wakeda, Y. J. Wang, and S. Ogata, npj Comput. Mater. **2**, 16013 (2016).
47 M. T. Sandor, H. B. Ke, W. H. Wang, and Y. Wu, J. Phys.-Condens. Matter **25**, 165701 (2013).
48 C. C. Yuan, J. F. Xiang, X. K. Xi, and W. H. Wang, Phys. Rev. Lett. **107**, 236403 (2011).